Metabolic Syndrome Interferes with Packaging of Proteins within Porcine Mesenchymal Stem Cell-Derived Extracellular Vesicles

ALFONSO EIRIN,[a] XIANG-YANG ZHU,[a] JOHN R. WOOLLARD,[a] HUI TANG,[a] SURENDRA DASARI,[b] AMIR LERMAN,[c] LILACH O. LERMAN [iD][a]

[a]Divisions of Nephrology and Hypertension, Mayo Clinic, Rochester, Minnesota, USA; [b]Health Sciences Research, Mayo Clinic, Rochester, Minnesota, USA; [c]Cardiovascular Diseases, Mayo Clinic, Rochester, Minnesota, USA

Correspondence: Lilach O. Lerman, M.D., Ph.D., Division of Nephrology and Hypertension, Mayo Clinic, 200 First Street SW, Rochester, Minnesota 55905, USA. Telephone: 507-266-9376; e-mail: lerman. lilach@mayo.edu

ABSTRACT

Mesenchymal stem/stromal cells (MSCs) release extracellular vesicles (EVs), which shuttle proteins to recipient cells, promoting cellular repair. We hypothesized that cardiovascular risk factors may alter the pattern of proteins packed within MSC-derived EVs. To test this, we compared the protein cargo of EVs to their parent MSCs in pigs with metabolic syndrome (MetS) and Lean controls. Porcine MSCs were harvested from abdominal fat after 16 weeks of Lean- or MetS-diet (n = 5 each), and their EVs isolated. Following liquid chromatography mass spectrometry proteomic analysis, proteins were classified based on cellular component, molecular function, and protein class. Five candidate proteins were validated by Western blot. Clustering analysis was performed to identify primary functional categories of proteins enriched in or excluded from EVs. Proteomics analysis identified 6,690 and 6,790 distinct proteins in Lean- and MetS-EVs, respectively. Differential expression analysis revealed that 146 proteins were upregulated and 273 downregulated in Lean-EVs versus Lean-MSCs, whereas 787 proteins were upregulated and 185 downregulated in MetS-EVs versus MetS-MSCs. Proteins enriched in both Lean- and MetS-EVs participate in vesicle-mediated transport and cell-to-cell communication. Proteins enriched exclusively in Lean-EVs modulate pathways related to the MSC reparative capacity, including cell proliferation, differentiation, and activation, as well as transforming growth factor-β signaling. Contrarily, proteins enriched only in MetS-EVs are linked to proinflammatory pathways, including acute inflammatory response, leukocyte transendothelial migration, and cytokine production. Coculture with MetS-EVs increased renal tubular cell inflammation. MetS alters the protein cargo of porcine MSC-derived EVs, selectively packaging specific proinflammatory signatures that may impair their ability to repair damaged tissues. STEM CELLS TRANSLATIONAL MEDICINE 2019;8:430–440

SIGNIFICANCE STATEMENT

This study found that metabolic syndrome (MetS) interferes with the packaging of proteins into porcine mesenchymal stem cell (MSC)-derived extracellular vesicles (EVs), favoring the inclusion of proinflammatory signatures that may impair the ability of MSCs to repair damaged tissues. These observations mandate caution during administration of autologous MSCs in subjects with MetS, and support development of strategies to improve the efficacy of MSCs and their EVs.

INTRODUCTION

Over the last decade, stem cell therapy has rapidly evolved to become a reality for therapeutic use in patients. There are currently hundreds of registered clinical trials testing the safety and efficacy of stem cells in a myriad of diseases (clinicalTrials.gov), and the number is expected to increase in the next few years. Mesenchymal stem/stromal cells (MSCs) have been particularly useful, partly because they have potent proangiogenic and immunomodulatory properties, can differentiate into a broad spectrum of cell linages, and can be obtained relatively easily from several tissue sources, including adipose tissue [1].

One of the primary mechanisms of action of MSCs relies on their ability to release extracellular vesicles (EVs), which include secreted membrane-enclosed microparticles like exosomes and microvesicles [2]. MSC-derived EVs carry genetic and protein content cargo that instigates a repair program in recipient cells, acting as the intermediary of the MSC paracrine function [3, 4]. In line with this, we have previously shown that EVs isolated from porcine

adipose tissue-derived MSCs contain multiple mRNAs, microRNAs, and proteins that participate in several cellular pathways, including angiogenesis, adipogenesis, inflammation, cellular transport, apoptosis, and transforming growth factor (TGF)-β signaling [5–7].

In addition to their function as endogenous mediators of intercellular communication, over the past few years experimental studies have uncovered protective roles of exogenously delivered MSC-derived EVs in multiple conditions, positioning EVs as a safe and effective stem cell-free alternative therapeutic intervention [8–10]. Hence, clinical trials are currently testing the safety and reparative capacity of autologous MSC-derived EVs (e.g., NCT02138331). However, many patients undergoing autologous therapy with autologous MSCs or MSC-derived EVs have coexisting cardiovascular risk factors, including obesity, hypertension, diabetes, and hyperlipidemia, which may cluster as the metabolic syndrome (MetS). Elucidating the potential impact of MetS on the paracrine function of MSCs may shed light on MSC biology and direct the therapeutic use of their EVs.

We have recently shown that MetS alters mRNA expression related to insulin signaling in porcine adipose tissue-derived MSCs [11], and interferes with the microRNA cargo of their EVs, favoring modulation of pathways involved in the development of MetS and its complications [12]. Notably, delivery of genetic material to recipient cells may constitute a different mode of regulation compared with protein delivery. However, whether MetS-induced modulation of protein-coding genes in MSCs alters the expression of proteins packed within their daughter EVs remains unknown. We hypothesized that MetS alters the protein content of EVs isolated from porcine adipose tissue-derived MSCs. To test this, we used liquid chromatography mass spectrometry (LC–MS/MS) proteomic analysis to characterize and compare the protein cargo of Lean- and MetS-MSCs to their EVs progeny.

MATERIALS AND METHODS

Experimental Design

Animal studies were performed with the approval of the Institutional Animal Care and Use Committee. Three-month-old premenstrual female domestic pigs were randomized into Lean or MetS groups (n = 5 each). Lean pigs were fed a standard chow, whereas MetS pigs were fed a high-cholesterol/carbohydrate diet (17% protein, 20% fructose, 20% complex carbohydrates, and 43% fat, supplemented with 2% cholesterol and 0.7% sodium cholate by weight) [13] for a total of 16 weeks.

After 16 weeks of Lean- or MetS-diet, body weight, mean arterial blood pressure, total cholesterol, low-density lipoprotein, triglyceride, fasting glucose, and insulin levels were measured, and insulin resistance was assessed by the homeostasis model assessment of insulin resistance (HOMA-IR) index. Animals were then euthanized with a lethal intravenous dose of sodium pentobarbital (100 mg/kg, Fatal Plus, Vortech Pharmaceuticals, Dearborn, MI), and subcutaneous abdominal fat (5–10 g) collected for MSC isolation [11, 14].

MSC and EV Characterization and Culture

MSCs were isolated from subcutaneous abdominal fat, digested in collagenase-H, filtered, and cultured for 3 weeks in advanced minimum essential medium (MEM) medium (Gibco/Invitrogen, Grand Island, NY) supplemented with 5% platelet lysate (PLTmax, Mill Creek Life Sciences, Rochester, MN) in 37°/5% CO_2, as

previously described [5, 15, 16]. The third passage was collected and kept in Gibco Cell Culture Freezing Medium for subsequent studies. Lean- and MetS-MSCs expressed common MSC markers (e.g., CD44, CD90, and CD105), and differentiated into osteocytes, chondrocytes, and adipocytes, as previously described [17–19], consistent with our observations in human MSCs [20].

Lean- and MetS-EVs were harvested from supernatants of their parent MSCs after a series of centrifugations and ultra-centrifugations [5–7]. A total of 10×10^6 MSCs were cultured for 48 hours in advanced MEM medium without any supplements and centrifuged at 2,000 g. Cell-free supernatants were then subjected to a second ultra-centrifugation at 100,000g for 1 hour at 4°C, washed in serum-free medium containing HEPES 25 mM, and submitted to a third step of ultra-centrifugation. Lean- and MetS-EVs exhibited typical size distribution by nanoparticle tracking analysis, and expressed common MSC and EV (e.g., CD9, CD29, CD81, and CD63) markers by Western blotting and fluorescence-activated cell sorting, as previously shown [6, 7, 9, 12, 21].

EV morphology was assessed in Lean- and MetS-EVs using a digital electron microscopy (Philips CM10 Transmission Electron Microscope). Samples fixed with Trump's fixative were processed at the Mayo Clinic's electron microscopy core facility. For electron microscopy analysis, five MSCs/group were randomly selected for examination. EV diameter and area were measured in 10 representative EVs in these cells using the straight and freehand tools of the National Institutes of Health Image-J software v1.44 (https://imagej.nih.gov/ij/), and averaged for each cell.

Proteomic Profiling and Network Pathway Analysis

LC–MS/MS proteomic analysis was performed, as previously described [6, 7, 22, 23]. Lean- and MetS-MSCs and EV pellets were solubilized in Tris buffer with 1% SDS HALT protease inhibitor and Benzonase. Rapid vortexing and three consecutive 5-minute incubations on ice were performed to achieve lysis, and protein samples were denatured by incubation at 85°C for 10 minutes. Aliquots (20 µg protein) were dried down, resolubilized in reducing sample buffer, and electrophoresed in 4%–20% TGX Ready gels (200 V for 30 minutes).

Lean- and MetS-gels were divided into seven horizontal regions, which were common to all samples. Sample lanes were duplicated, and individual gel sections digested by overnight incubation at 37°C with 140 ng of trypsin dissolved in 25 mM Tris (pH 8.2) [23]. Peptides were then extracted with 30 µl of 50% acetonitrile in 4% trifluoroacetic acid, evaporated to dryness on a vacuum concentrator, and stored at −80°C for subsequent analysis. Peptide extracts were reconstituted and aliquots of the peptide extracts loaded onto a 0.25 µl bed OptiPak trap (Optimize Technologies, Oregon City, Oregon), washed and transferred onto a 35 cm × 100 µm PicoFrit column-9, using a Dionex UltiMate 3000 Rapid Separation Liquid Chromatography (RSLC) LC system (Thermo-Fisher Scientific, Waltham, MA). Peptides were then separated using a 400 nl/minute LC gradient, held at 95%B for 8 minutes, and re-equilibrated to 2%B. Eluting peptides were analyzed using a QExactive mass spectrometer (Thermo-Fisher Scientific), as described [6, 7].

A label-free peptide MS1 intensity-based method was used to identify differentially expressed proteins between MSCs and EVs. MaxQuant (version 1.5.1) software was used to obtain a list of proteins and their corresponding intensities in each MSC and EV sample [24]. Differential expression analysis was performed

after the data was normalized by protein loading, and differential *p*-values false discovery rates (FDR) corrected [25]. Proteins with an FDR < 0.05 and log2 fold-change (EVs/MSCs) > 2 were classified as enriched in EVs, whereas those with FDR < 0.05 and log2 fold-change < −2 were considered as excluded. Differentially expressed proteins were classified by their cellular component, molecular function, and class using Protein Analysis Through Evolutionary Relationships [26]. Functional pathway analysis was performed using the Database for Annotation and Integrated Discovery (DAVID 6.8) [27].

Validation of Proteomic Analysis

Remodeling And Spacing Factor (RSF)-1, Transforming Growth Factor β Receptor (TGFBR)-2, ACVR-1, Tumor Necrosis Factor Superfamily Member (TNFSF)-9, and Von Willebrand Factor (VWF) proteins were selected for validation, and their expression in EVs and MSCs (*n* = 5 each) measured by Western blot (Abcam, ab83322, 1:1,000; Abcam, ab61213, 1:1,000; lsbio, LS-B3020, 1:1,000; Abcam, ab64912, 1:1,000; and Abcam, ab6994, 1:500, respectively).

MSC-Derived EV Effects on Renal Tubular Cells

Pig proximal kidney tubular epithelial cells (LLC-PK1, ATCC, Manassas) were cultured in Medium-199 (Gibco BRL) containing 3% FBS [19] alone or cocultured with Lean- and MetS-MSC-derived EVs (5 μg of EV protein, *n* = 5 each). Proliferation of confluent PK1 cells was evaluated by calculating the doubling time of cell numbers between the second and third passages using an online formula (http://www.doubling-time.com/compute.php), as previously described [28]. Nuclear translocation of the proinflammatory transcription factor nuclear factor (NF)-kB was evaluated in tubular epithelial cells by immunofluorescent staining (Abcam, 1:200, Cambridge, MA). Nuclear DNA was stained with 4′, 6-diamidino-2-phenylindole (DAPI). Double positive (NFkB/DAPI) areas were quantified in 15–20 random fields using a computer-aided image analysis program (ZEN 2012 blue edition; Carl Zeiss SMT, Oberkochen, Germany), and the results from all fields were averaged. Tubular epithelial cell inflammation was evaluated by immunofluorescent staining with antibodies against tumor necrosis factor (TNF)-α (Santa Cruz Biotechnology Inc., Santa Cruz, CA, 1:200), monocyte chemoattractant protein (MCP)-1, interleukin (IL)-6, and IL-1β (MyBioSource, San Diego, CA, http://www.mybiosource.com 1:7,500).

Statistical Analysis

Statistical analysis was performed using JMP 13.0 (SAS Institute, Cary, NC). Data were expressed as mean ± SD. Unpaired Student's *t* test was used to evaluate statistically significant differences between the Lean and MetS groups. Comparisons within PK1, PK1 + Lean-EVs, and PK1 + MetS-EVs were performed using analysis of variance followed by the unpaired Student's *t* test. Statistical significance was accepted if *p* < .05.

RESULTS

Systemic Characteristics

At the end of the study and completion of 16 weeks of diet, MetS pigs successfully developed MetS, reflected in increased body weight, blood pressure, cholesterol fractions, and triglyceride levels (Table 1). Although fasting glucose levels did not

Table 1. Systemic measurements (mean ± SD) in domestic pigs after 16 weeks of lean or MetS diet (*n* = 5 each)

Parameter	Lean	MetS
Body weight (kg)	72.1 ± 12.0	92.1 ± 2.4*
Mean blood pressure (mmHg)	99.4 ± 11.8	125.6 ± 8.2*
Total cholesterol (mg/dl)	83.5 ± 7.6	432.9 ± 88.4*
LDL cholesterol (mg/dl)	34.0 ± 7.5	401.2 ± 148.2*
Triglycerides (mg/dl)	7.6 ± 1.9	15.8 ± 4.3*
Fasting glucose (mg/dl)	123.6 ± 18.5	116.0 ± 20.4
Fasting insulin (μU/ml)	0.4 ± 0.1	0.7 ± 0.1*
HOMA-IR score	0.6 ± 0.1	1.8 ± 0.4*

*p < .05 versus Lean.
Abbreviations: HDL, high-density lipoprotein; LDL, low-density lipoprotein; HOMA-IR, homeostasis model assessment of insulin resistance.

differ between the groups, fasting insulin levels and HOMA-IR score were higher in MetS compared with Lean pigs.

MSC and EV Characterization and Culture

Electron microscopy analysis revealed comparable morphology of Lean- and MetS-EVs (Supporting Information Fig. S1A). EV diameter and area were also similar between the groups (Supporting Information Fig. S1B).

Identification and Distribution of Differentially Expressed Proteins

Proteomics analysis identified a total of 6,690 and 6,790 distinct protein groups in Lean- and MetS-EVs, respectively, with molecular weights ranging from 10 to 250 kDa (Supporting Information Fig. S2).

Differential expression analysis revealed that 146 proteins were upregulated and 273 downregulated in Lean-EVs compared with Lean-MSCs, whereas 185 proteins were upregulated and 787 downregulated in MetS-EVs compared with MetS-MSCs (Fig. 1A).

Proteins Enriched in Both Lean- and MetS-EVs

Only 55 proteins were enriched in both Lean- and MetS-EVs (Figs. 1B, 2A). These proteins were equally distributed in cellular, extracellular, and membrane compartments (Fig. 2B). These are mostly hydrolases, signaling molecules, and transporters with catalytic, binding, and channel regulator activity, primarily implicated in vesicle-mediated transport and cell-to-cell communication (e.g., secretion, adhesion, plasma membrane), as well as in vascular development (Fig. 2C).

Proteins Enriched Only in Lean-EVs

Ninety-one proteins were exclusively enriched in Lean-EVs (Figs. 1B, 3A), including cellular, extracellular, and membrane proteins with transporter, binding, and catalytic activity (Fig. 3B). These are primarily transporters, receptors, and hydrolases that modulate several cellular pathways related to the MSC reparative capacity, including, cell proliferation, differentiation, division, and activation, as well as TGF-β signaling (Fig. 3C).

Proteins Enriched Only in MetS-EVs

A total of 130 proteins were enriched only in MetS-EVs (Figs. 1B, 4A), with a larger proportion of extracellular proteins,
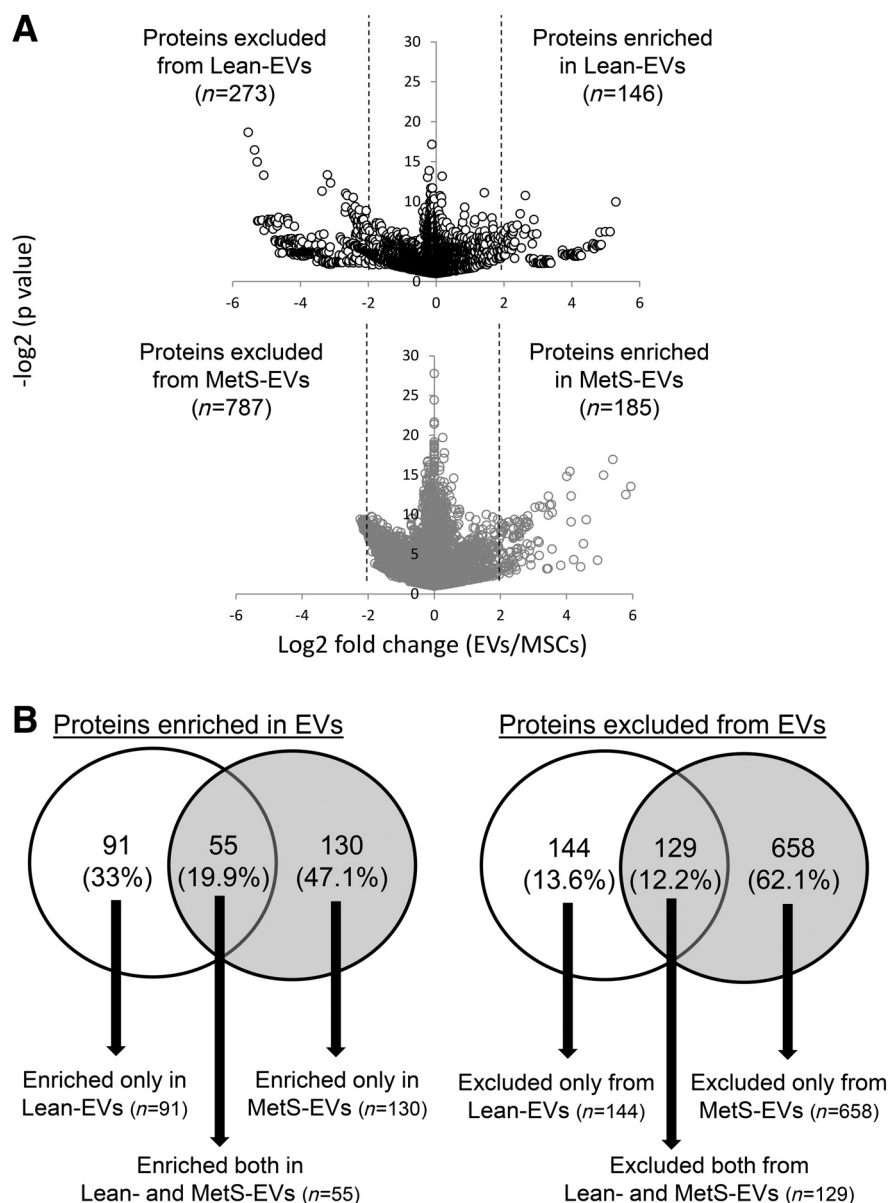
Figure 1. **(A):** Volcano plot of identified proteins enriched in or excluded from Lean- (top) and metabolic syndrome-extracellular vesicles (MetS-EVs; bottom). A total of 146 proteins were enriched in lean- and 185 in MetS-EVs compared with their parent mesenchymal stem/stromal cells (MSCs), whereas 273 proteins were excluded from Lean- and 787 from MetS-EVs. **(B):** Venn diagrams showing distribution of proteins enriched in (left) or excluded from (right) Lean- and MetS-EVs.

less transporter function, but slightly more catalytic activity compared with those enriched only in Lean-EVs (Fig. 4B). They have more enzyme modulator and signaling molecule activity compared with their Lean counterparts, as well as an important proinflammatory component with several inflammation-related categories, including, acute inflammatory response, activation of immune response, complement, regulation of immune response, leukocyte transendothelial migration, and regulation of cytokine production (Fig. 4C).

Proteins Excluded from EVs

Proteins excluded from both Lean and MetS-EVs (n = 129) and those excluded only from Lean- (n = 144) and MetS- (n = 658) EVs are nuclear and nucleolar proteins primarily involved in

transcription, RNA binding, and splicing (Fig. 1B; Supporting Information Fig. S3A–S3C). More proteins related to RNA processing, nucleolus, and nuclear transport, were excluded from MetS-EV compared with Lean-EV.

The data generated in this study have been deposited in the mass spectrometry interactive virtual environment (MassIVE, accession number MSV000081944).

Validation of Proteomic Analysis

Expression of the candidate proteins followed the same patterns as the proteomics findings. Specifically, RSF-1 was higher in Lean- and MetS-EVs compared with their parent MSCs, TGFBR-2, and ACVR1 were higher in Lean-EVs compared with Lean-MSCs, whereas
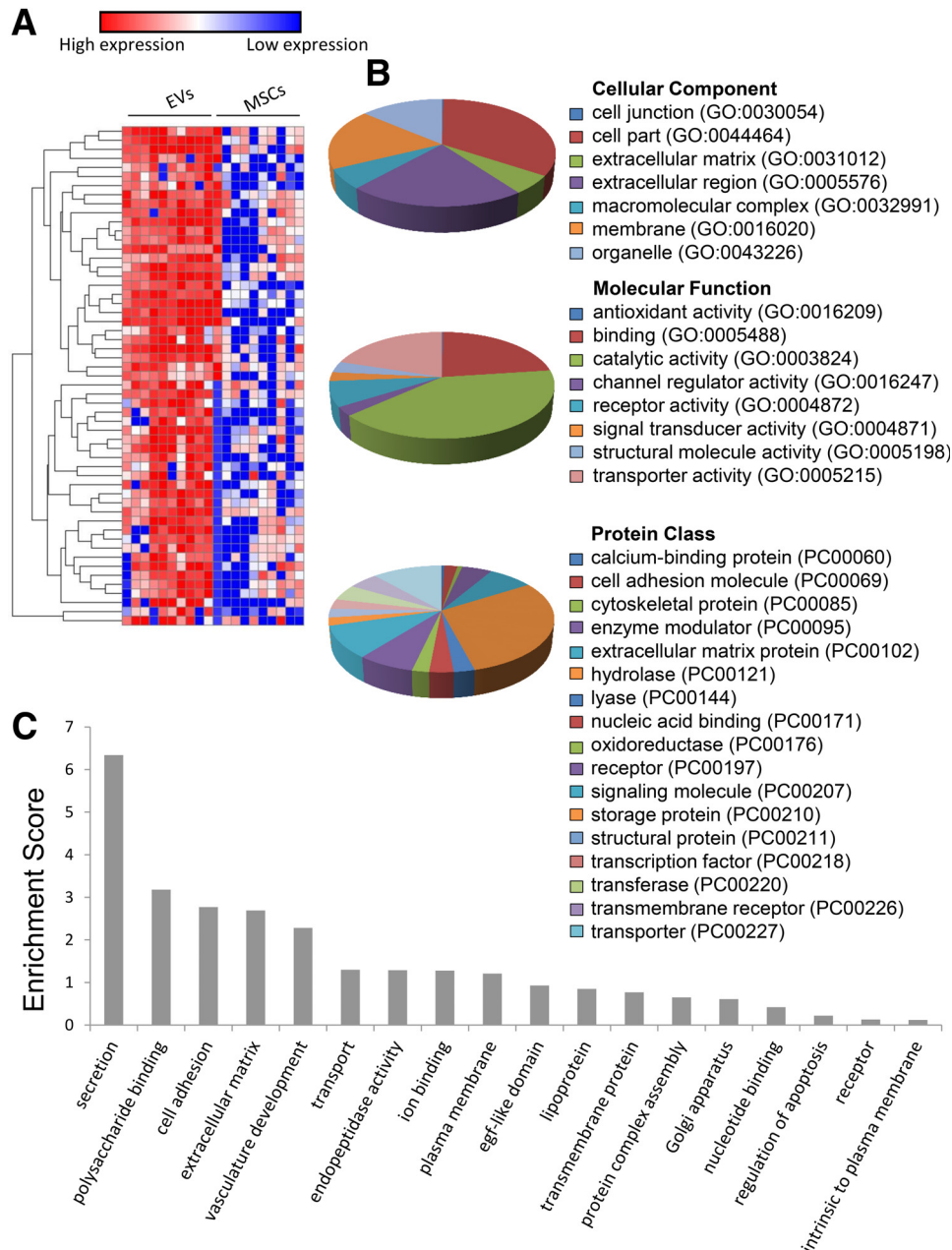
Figure 2. **(A):** Heat map of 55 proteins enriched both in Lean- and metabolic syndrome-extracellular vesicles (MetS-EVs) compared with their parent mesenchymal stem/stromal cells. **(B):** Panther analysis of cellular component, molecular function, and protein class of proteins enriched both in Lean- and MetS-EVs. **(C):** Functional annotation clustering (using DAVID 6.8) of proteins enriched both in Lean- and MetS-EVs.

TNSFF9 and VWF were higher in MetS-EVs compared with MetS-MSCs (Supporting Information Fig. S4).

MetS-EVs Increased Renal Tubular Cell Inflammation

Proliferation capacity (doubling time) of PK1 cells was similar following coincubation with Lean- or MetS-EVs (Supporting Information Fig. S5). In untreated tubular epithelial cells, NFkB was localized predominantly in the cytoplasm. Cocultured with Lean-EVs has no effect on NFkB localization, whereas coculture with MetS-EVs induced NFkB nuclear translocation (Fig. 5). Furthermore, coculture with MetS-EVs induced in PK1 a greater

expression of TNF-α, MCP-1, IL-6, and IL-1β compared with untreated cells or cells cocultured with Lean-EVs (Fig. 6).

DISCUSSION

The current study shows that MetS alters the protein cargo of porcine MSC-derived EVs. Our analysis demonstrates that proteins enriched in both Lean- and MetS-EVs participate in vesicle-mediated transport and cell-to-cell communication. Proteins enriched exclusively in Lean-EVs modulate pathways related to the MSC reparative capacity, whereas those enriched only in
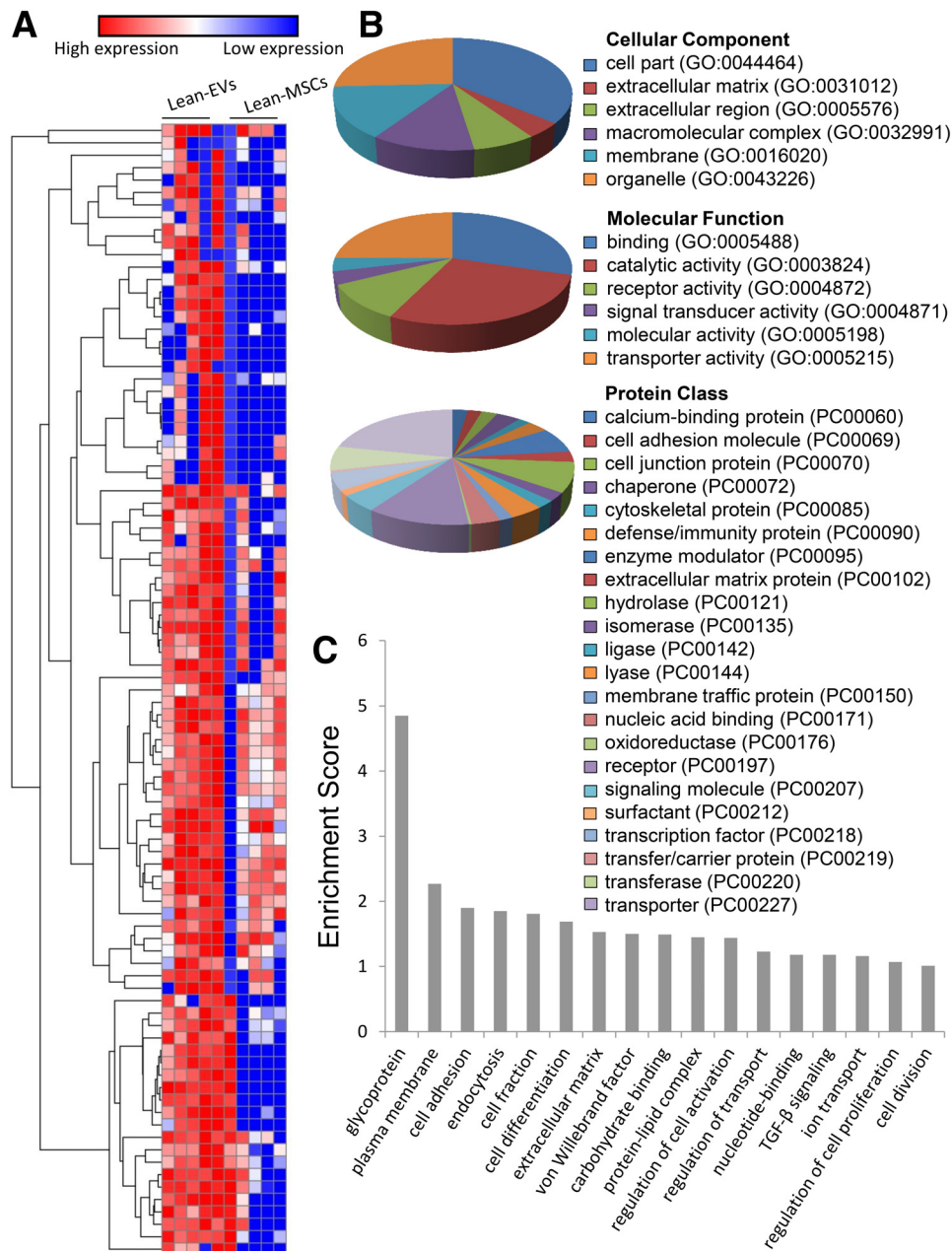
Figure 3. **(A):** Heat map of 91 proteins enriched only in Lean-extracellular vesicles (EVs). **(B):** Panther analysis of cellular component, molecular function, and protein class of proteins enriched only in Lean-EVs. **(C):** Functional annotation clustering (using DAVID 6.8) of proteins enriched only in Lean-EVs.

MetS-EVs are linked to several proinflammatory pathways. Indeed, tubular cells coincubated with MetS-EVs showed increased NF-kB nuclear translocation, reflecting NF-kB activation. These observations indicate that MetS alters packaging of proteins into porcine MSC-derived EVs, favoring the inclusion of pro-inflammatory signatures that may impair the ability of MSCs to repair damaged tissues.

Endowed with unique self-renewal and proliferative capacity, and important proangiogenic and immunomodulatory properties, MSCs are currently positioned as the primary stem-cell option for regenerative therapy [1]. In recent years, clinical trials have demonstrated the safety and efficacy of this approach to treat several diseases. Furthermore, preclinical studies have shown that the primary mechanism of action of MSCs is paracrine release of EVs, which transfer genes, proteins, and microRNA to recipient cells, promoting tissue repair [3, 4]. However, many patients that might benefit from MSC therapy are exposed to coexisting cardiovascular risk factors, which may potentially alter the protein cargo of EVs. To test this postulation, the current study characterized and compared the protein cargo of EVs harvested from Lean- and MetS-adipose tissue-derived MSCs.

Our proteomic analysis identified higher average protein expression in both Lean- and MetS-MSCs than in their respective EVs, consistent with our previous observations [6, 7]. Although
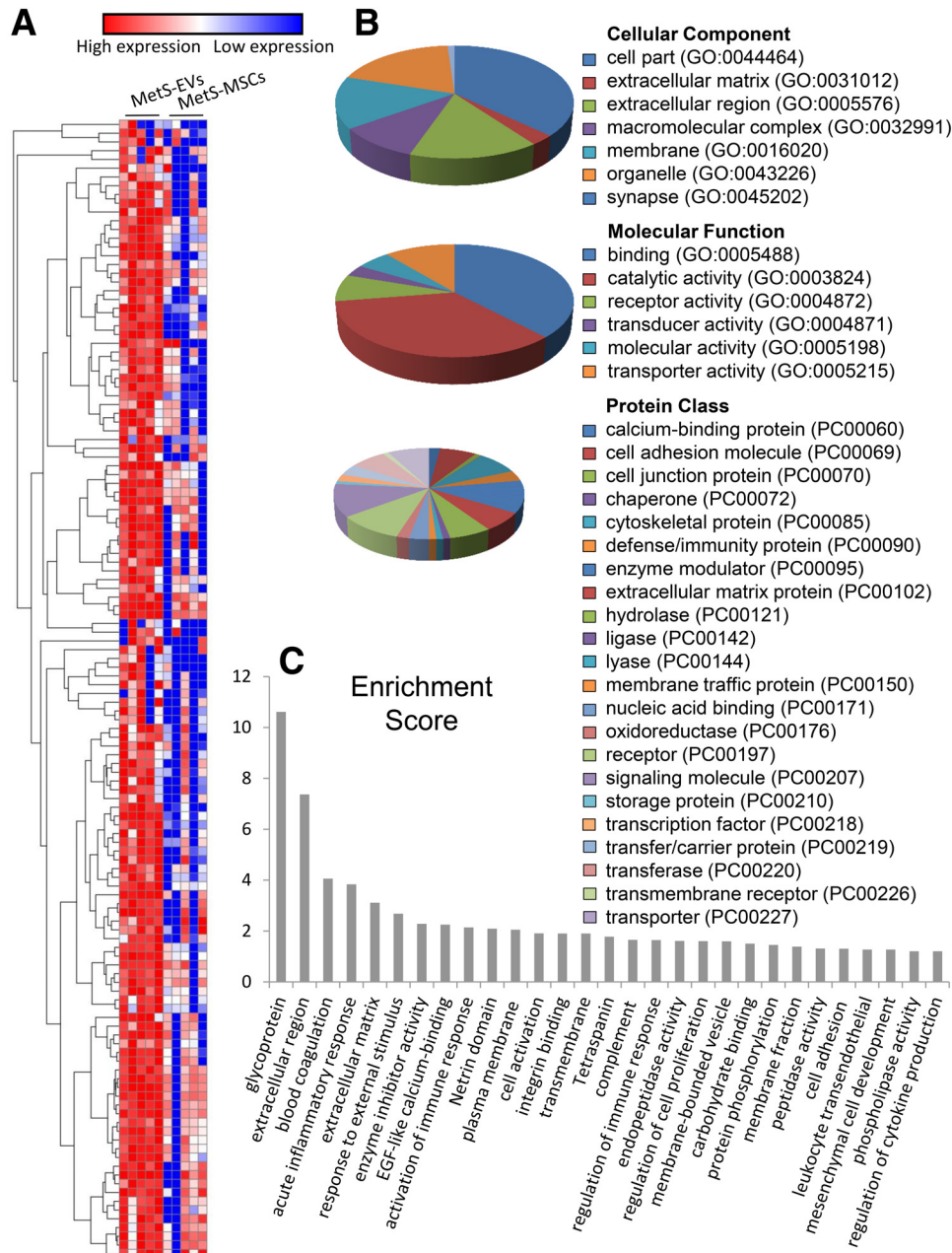
Figure 4. **(A):** Heat map of 130 proteins enriched only in metabolic syndrome-extracellular vesicles (MetS-EVs). **(B):** Panther analysis of cellular component, molecular function, and protein class of proteins enriched only in MetS-EVs. **(C):** Functional annotation clustering (using DAVID 6.8) of proteins enriched only in MetS-EVs.

protein expression was higher in MetS- compared with Lean-MSCs, EV protein expression was similar between the groups, suggesting that MetS-MSCs pack a smaller proportion of proteins into their EVs. Analysis of proteins enriched in Lean- and MetS-EVs relative to their parent MSCs revealed three distinct protein enrichment categories: those enriched in both Lean- and MetS-EVs, exclusively in Lean-EVs, or only in MetS-EVs. Interestingly, functional annotation clustering analysis indicates that these protein groups exert disparate functions.

Proteins enriched both in Lean- and MetS-EVs primarily participate in vesicle-mediated transport and cell-to-cell communication, including modulation of cell secretion, adhesion, and transport, as well as proteins intrinsic to the plasma membrane. We have previously shown that porcine MSC-derived EVs transport multiple genes and micro-RNAs that participate in cellular transport [5]. The current study extends these observations to demonstrate that proteins enriched both in Lean- and MetS-EVs are also implicated in cellular transport. For example, Lean- and MetS-EVs contain the cell adhesion protein amine oxidase copper-containing-3, also known as vascular adhesion protein-1, which mediates adhesion of lymphocytes to endothelial cells [29]. In addittion, Lean- and MetS-EVs are enriched with several transmembrane transport proteins (e.g., ATPase and H+/K+ exchanging α polypeptide), suggesting that both Lean- and MetS-EVs serve as fundamental
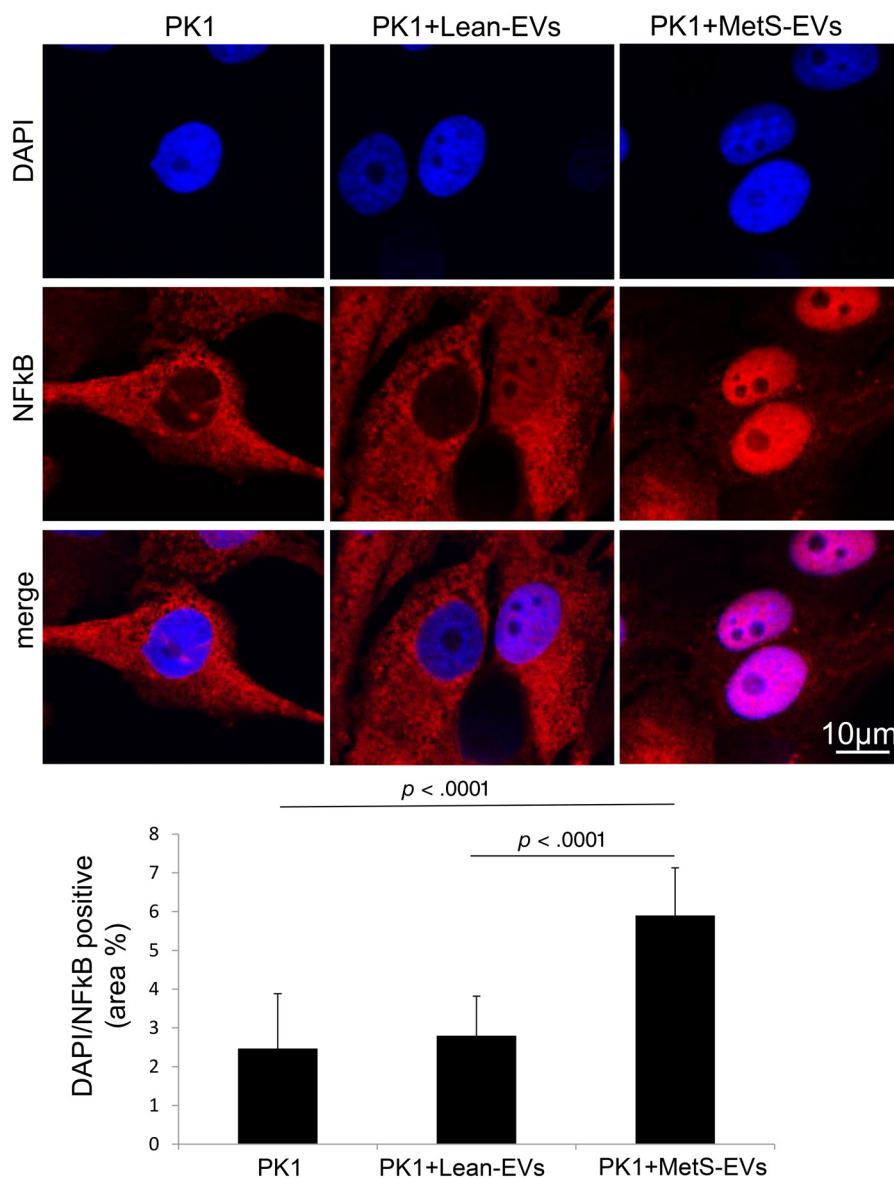
Figure 5. Immunofluorescence staining showing subcellular distribution of nuclear factor (NF)-kB in renal tubular epithelial cells (PK1) untreated or treated with lean- and metabolic syndrome-extracellular vesicles (MetS-EVs). MetS-EVs induced a marked translocation of NFkB from the cytoplasm to the cellular nucleus ($n = 5$ each).

vehicles for transfer of genetic and protein content mediating intercellular communication.

Furthermore, a significant proportion of proteins enriched in Lean- and MetS-EVs contribute to vascular development. This category includes angiopoietin-like-4, cysteine-rich angiogenic inducer-61, and protein tyrosine phosphatase receptor type-J, a member of the protein tyrosine phosphatase family that acts as an important driver of vascular endothelial growth factor (VEGF)-dependent angiogenesis [30]. Lean- and MetS-EVs also contain protein tyrosine phosphatase nonreceptor type-6, a member of the protein tyrosine phosphatase family that functions as an important regulator of angiogenesis through VEGF receptor-2 signaling pathway [31]. Therefore, despite differences in protein content, our observations suggest that MetS-MSCs may preserve their proangiogenic capabilities.

Proteins enriched exclusively in Lean-EVs modulate pathways related to the MSC reparative capacity, including cell proliferation, differentiation, division, and activation, as well as TGF-β signaling. Among them are glycoproteins and cyclin-dependent kinases which function in adhesion, signal transduction and, proliferation of several cell lines, including neurons, erythrocytes, and myeloid cells. For example, the glycoprotein integrin α-1, highly enriched in Lean-EVs, heterodimerizes with the β-1 subunit to form a cell-surface receptor for collagen and laminin. Likewise, cyclin-dependent kinase-2 acts in complex with cyclin-A2 in the cell cycle to promote cell proliferation [32]. In addition, proteins that modulate the frequency, rate, or extent of cell activation are present in Lean-EVs, including the type-II transmembrane glycoprotein CD38. It has been shown that MSCs modulates B-cell apoptosis by increasing the
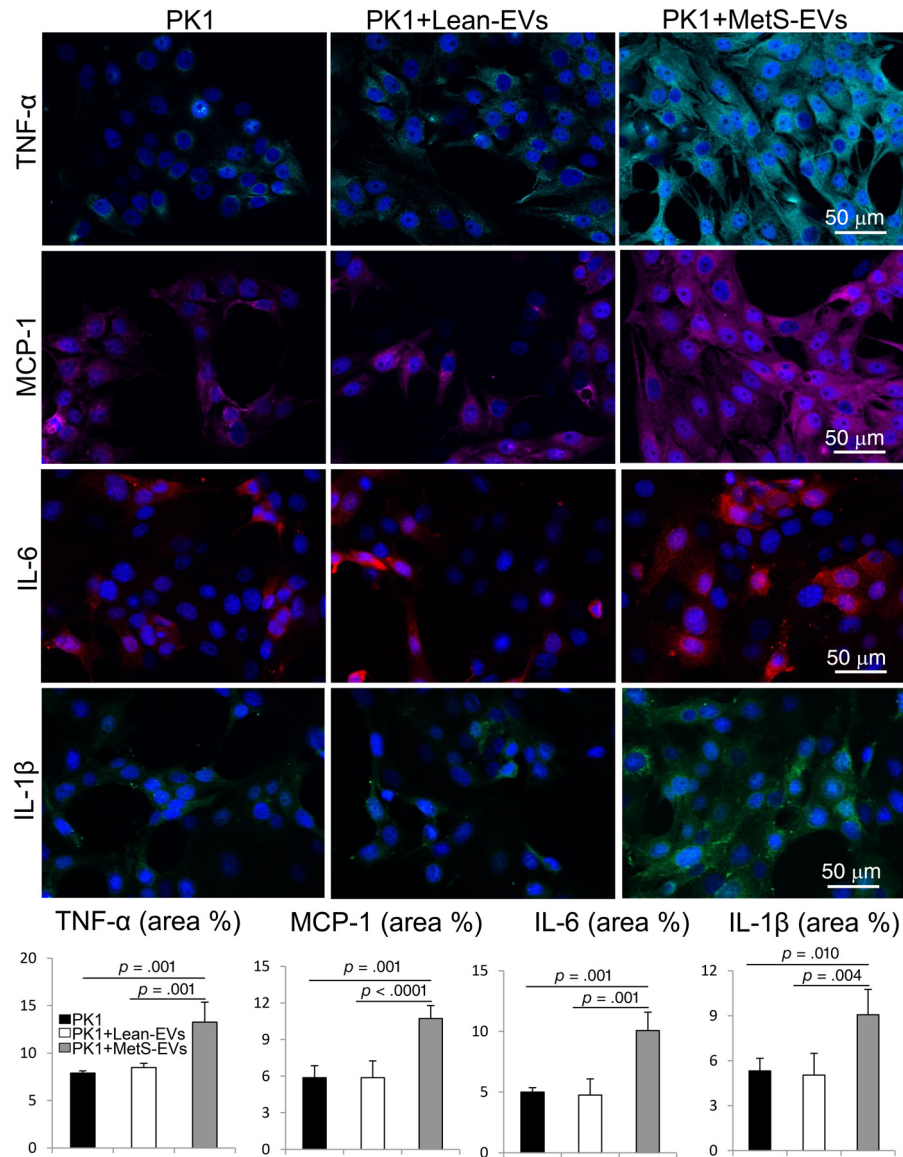
Figure 6. Expression of tumor necrosis factor (TNF)-α, monocyte chemoattractant protein (MCP)-1, interleukin (IL)-6, and IL-1β was similar in PK1 and PK1 + Lean-extracellular vesicles (EVs), but higher in PK1 + metabolic syndrome-EVs compared with PK1 or PK1 + Lean-EVs (n = 5 each).

expression of CD38, associated with activation of signal molecules in MSCs [33]. Therefore, our findings suggest that EVs might mediate the "crosstalk" between MSCs and B-cells, resulting in activation features for both cell populations.

Lean-EVs are also enriched with several proteins that modulate TGF-β signaling, including TGFBR-2, TGFBR-3, and Inhibin β-A, consistent with our previous finding that EVs contain high levels of genes and protein ligands within the TGF-β family [5, 6]. TGF-β superfamily has crucial roles in tissue development and differentiation, and modulates proliferation and differentiation of MSCs, acting as autocrine signals to sustain MSC function [34]. TGF-β signaling also induces regulatory T-cells and suppresses inflammation [35]. Collectively, these observations suggest that EVs produced by Lean-MSCs might mitigate cellular injury by modulating multiple reparative pathways. Current evidence suggests that MSC possess potent immunomodulatory properties that are primarily mediated by the release of EVs

[36], which carry anti-inflammatory elements in the form of genes, proteins, and microRNAs [8, 37]. Furthermore, we have recently shown that knocking down the anti-inflammatory gene IL-10 in MSC-derived EVs blunts their capacity to repair the post-stenotic kidney, implying that the salutary effects of EVs are mediated by their anti-inflammatory cargo [9].

Contrarily, we found that proteins enriched only in MetS-EVs are linked to several proinflammatory pathways, including acute inflammatory response, leukocyte transendothelial migration, and cytokine production, including platelet and endothelial cell adhesion molecule (PECAM)-1, IL-1α, IL-6, and several components of the complement system. PECAM-1 is a member of the immunoglobulin superfamily involved in leukocyte migration, and integrin activation, whereas the proinflammatory cytokine IL-1α is involved in several immune responses, such as inflammatory cell maturation and proliferation. IL-6 is also implicated in several inflammation-associated disease states, and its activation

is induced by tumor necrosis factor (TNF)-α [38]. We have previously shown that MetS-MSCs showed increased senescence compared with Lean-MSCs, associated with enhanced adipogenic and osteogenic propensity, which were partly mediated by upregulated TNF-α [28]. Therefore, our observations suggest that MetS may impede the anti-inflammatory capacity of MSCs and their EVs, blunting their potential to repair damaged tissues.

We have previously found that nuclear proteins are largely excluded from EV cargo [6]. The present study shows that nuclear and nucleolar proteins primarily involved in transcription, RNA binding, and splicing, are also excluded from MetS-EVs, implying that MetS does not prominently interfere with selective exclusion of proteins from MSC-derived EVs. Nevertheless, more proteins related to RNA processing, nucleolus, and nuclear transport, were excluded from MetS-EV compared with Lean-EV. Future studies are needed to elucidate the mechanisms underlying the selective exclusion of these proteins into MSC-derived EVs.

To determine whether these differences in overall protein cargo between Lean- and MetS-EVs affect their immunomodulatory potential, we compared nuclear and cytoplasmic distribution of NF-kB in renal tubular epithelial cells untreated or cocultured with Lean- or MetS-EVs. This transcription factor regulates several aspects of innate and adaptive immunity, and its nuclear translocation is a key step for triggering a proinflammatory response [39]. in vitro studies have shown that MSCs obtained from healthy donor bone marrow secrete anti-inflammatory proteins, which attenuate inflammation by preventing NFkB nuclear translocation [40]. In the current study, we found that similar to untreated cells, NFkB was distributed predominantly in the cytoplasm of tubular cells cocultured with Lean-EVs. Contrarily, coculture with MetS-EVs induced NFkB nuclear translocation, reflecting NF-kB activation. This may in turn induce expression of genes encoding for several proinflammatory cytokines, impairing the immunomodulatory potential of MSCs in subjects with MetS. Indeed, we found that expression of the proinflammatory cytokines TNF-α, MCP-1 IL-6, and IL-1β was higher in renal tubular cells cocultured with MetS-EVs compared with cells untreated or cocultured with Lean-EVs, extending our previous observations [41]. Nevertheless, proliferation capacity of PK1 cells was unaltered following coincubation with either Lean- or MetS-EVs, arguing against major effect of these inflammatory pathways on proliferation of renal tubular cells.

Our study is limited by a small sample size (*n* = 5 each) and short duration of MetS compared with the human disease. In addition, our model does not allow identifying the impact of each independent component of MetS on the protein cargo of MSC-derived EVs. Nevertheless, a high-cholesterol/carbohydrate diet for 16 weeks sufficed to achieve several features of human MetS and alter the protein content of MSC-derived EVs. Future studies are needed to explore whether these changes compromise the in vivo reparative capacity of MSCs and their daughter EVs.

CONCLUSION

We found that MetS modifies the protein cargo of porcine MSC-derived EVs. Some proteins enriched in both Lean- and MetS-EVs participate in fundamental vesicle-mediated transport and cell-to-cell communication, whereas a number of proteins are selectively enriched exclusively in either Lean- or MetS-EVs and modulate distinct cellular functions. Lean-EVs proteins modulate pathways related to the MSC reparative capacity, whereas those enriched only in MetS-EVs are linked to several proinflammatory pathways. Therefore, MetS alters the protein content of porcine MSC-derived EVs, preferentially packing proinflammatory proteins, which may compromise the reparative capacity of MSCs and their EVs both in the endogenous microenvironment and after autologous transplantation.

AUTHOR CONTRIBUTIONS

A.E.: conception and design, collection and/or assembly of data, data analysis and interpretation, manuscript writing, final approval of manuscript; X.-Y.Z., J.R.W., H.T., S.D., and A.L.: collection and/or assembly of data, data analysis and interpretation, final approval of manuscript; L.O.L.: conception and design, data analysis and interpretation, manuscript writing, final approval of manuscript.

DISCLOSURE OF POTENTIAL CONFLICTS OF INTEREST

The authors indicated no potential conflicts of interest.

REFERENCES

1   Dominici M, Le Blanc K, Mueller I et al. Minimal criteria for defining multipotent mesenchymal stromal cells. The International Society for Cellular Therapy position statement. Cytotherapy 2006;8:315–317.

2   Lotvall J, Hill AF, Hochberg F et al. Minimal experimental requirements for definition of extracellular vesicles and their functions: A position statement from the International Society for Extracellular Vesicles. J Extracell Vesicles 2014;3:26913.

3   Lai RC, Chen TS, Lim SK. Mesenchymal stem cell exosome: A novel stem cell-based therapy for cardiovascular disease. Regen Med 2011;6:481–492.

4   Yeo RW, Lai RC, Zhang B et al. Mesenchymal stem cell: An efficient mass producer of exosomes for drug delivery. Adv Drug Deliv Rev 2013;65:336–341.

5   Eirin A, Riester SM, Zhu XY et al. MicroRNA and mRNA cargo of extracellular vesicles from porcine adipose tissue-derived mesenchymal stem cells. Gene 2014;551:55–64.

6   Eirin A, Zhu XY, Puranik AS et al. Comparative proteomic analysis of extracellular vesicles isolated from porcine adipose tissue-derived mesenchymal stem/stromal cells. Sci Rep 2016;6: 36120.

7   Eirin A, Zhu XY, Puranik AS et al. Integrated transcriptomic and proteomic analysis of the molecular cargo of extracellular vesicles derived from porcine adipose tissue-derived

mesenchymal stem cells. PLoS One 2017;12: e0174303.

8   Nargesi AA, Lerman LO, Eirin A. Mesenchymal stem cell-derived extracellular vesicles for renal repair. Curr Gene Ther 2017;17: 29–42.

9   Eirin A, Zhu XY, Puranik AS et al. Mesenchymal stem cell-derived extracellular vesicles attenuate kidney inflammation. Kidney Int 2017;92:114–124.

10   Shigemoto-Kuroda T, Oh JY, Kim DK et al. MSC-derived extracellular vesicles attenuate immune responses in two autoimmune murine models: Type 1 diabetes and uveoretinitis. Stem Cell Rep 2017;8:1214–1225.

11   Conley SM, Zhu XY, Eirin A et al. Metabolic syndrome alters expression of insulin

signaling-related genes in swine mesenchymal stem cells. Gene 2018;644:101–106.

12 Meng Y, Eirin A, Zhu XY et al. The metabolic syndrome alters the miRNA signature of porcine adipose tissue-derived mesenchymal stem cells. Cytometry A 2017;93:93–103.

13 Pawar AS, Zhu XY, Eirin A et al. Adipose tissue remodeling in a novel domestic porcine model of diet-induced obesity. Obesity 2015;23:399–407.

14 Eirin A, Ebrahimi B, Zhang X et al. Mitochondrial protection restores renal function in swine atherosclerotic renovascular disease. Cardiovasc Res 2014;103:461–472.

15 Crespo-Diaz R, Behfar A, Butler GW et al. Platelet lysate consisting of a natural repair proteome supports human mesenchymal stem cell proliferation and chromosomal stability. Cell Transplant 2011;20:797–811.

16 Meng Y, Eirin A, Zhu XY et al. Obesity-induced mitochondrial dysfunction in porcine adipose tissue-derived mesenchymal stem cells. J Cell Physiol 2018;233:5926–5936.

17 Eirin A, Zhu XY, Krier JD et al. Adipose tissue-derived mesenchymal stem cells improve revascularization outcomes to restore renal function in swine atherosclerotic renal artery stenosis. Stem Cells 2012;30:1030–1041.

18 Ebrahimi B, Eirin A, Li Z et al. Mesenchymal stem cells improve medullary inflammation and fibrosis after revascularization of swine atherosclerotic renal artery stenosis. PLoS One 2013;8:e67474.

19 Zhu XY, Urbieta-Caceres V, Krier JD et al. Mesenchymal stem cells and endothelial progenitor cells decrease renal injury in experimental swine renal artery stenosis through different mechanisms. Stem Cells 2013;31:117–125.

20 Dudakovic A, Camilleri E, Riester SM et al. High-resolution molecular validation of self-renewal and spontaneous differentiation in clinical-grade adipose-tissue derived human mesenchymal stem cells. J Cell Biochem 2014; 115:1816–1828.

21 Eirin A, Zhu XY, Jonnada S et al. Mesenchymal stem cell-derived extracellular vesicles improve the renal microvasculature in metabolic renovascular disease in swine. Cell Transplant 2018;27:1080–1095.

22 Hogan MC, Johnson KL, Zenka RM et al. Subfractionation, characterization, and in-depth proteomic analysis of glomerular membrane vesicles in human urine. Kidney Int 2014;85: 1225–1237.

23 Hogan MC, Bakeberg JL, Gainullin VG et al. Identification of biomarkers for PKD1 using urinary exosomes. J Am Soc Nephrol 2015;26:1661–1670.

24 Cox J, Hein MY, Luber CA et al. Accurate proteome-wide label-free quantification by delayed normalization and maximal peptide ratio extraction, termed MaxLFQ. Mol Cell Proteomics 2014;13:2513–2526.

25 Kim KI, van de Wiel MA. Effects of dependence in high-dimensional multiple testing problems. BMC Bioinform 2008;9:114.

26 Mi H, Lazareva-Ulitsky B, Loo R et al. The PANTHER database of protein families, subfamilies, functions and pathways. Nucleic Acids Res 2005;33:D284–D288.

27 Huang d W, Sherman BT, Lempicki RA. Systematic and integrative analysis of large gene lists using DAVID bioinformatics resources. Nat Protoc 2009;4:44–57.

28 Zhu XY, Ma S, Eirin A et al. Functional plasticity of adipose-derived stromal cells during development of obesity. Stem Cells Translational Medicine 2016;5:893–900.

29 Alexander JS, Granger DN. Lymphocyte trafficking mediated by vascular adhesion protein-1: Implications for immune targeting and cardiovascular disease. Circ Res 2000;86: 1190–1192.

30 Fournier P, Dussault S, Fusco A et al. Tyrosine phosphatase PTPRJ/DEP-1 is an essential promoter of vascular permeability, angiogenesis, and tumor progression. Cancer Res 2016; 76:5080–5091.

31 Chu LY, Ramakrishnan DP, Silverstein RL. Thrombospondin-1 modulates VEGF signaling via CD36 by recruiting SHP-1 to VEGFR2 complex in microvascular endothelial cells. Blood 2013; 122:1822–1832.

32 Gopinathan L, Tan SL, Padmakumar VC et al. Loss of Cdk2 and cyclin A2 impairs cell proliferation and tumorigenesis. Cancer Res 2014;74:3870–3879.

33 Ding W, Nowakowski GS, Knox TR et al. Bi-directional activation between mesenchymal stem cells and CLL B-cells: Implication for CLL disease progression. Br J Haematol 2009; 147:471–483.

34 Scheel C, Eaton EN, Li SH et al. Paracrine and autocrine signals induce and maintain mesenchymal and stem cell states in the breast. Cell 2011;145:926–940.

35 Ansa-Addo EA, Zhang Y, Yang Y et al. Membrane-organizing protein moesin controls Treg differentiation and antitumor immunity via TGF-beta signaling. J Clin Invest 2017;127: 1321–1337.

36 Gao F, Chiu SM, Motan DA et al. Mesenchymal stem cells and immunomodulation: Current status and future prospects. Cell Death Dis 2016;7:e2062.

37 Aghajani Nargesi A, Lerman LO, Eirin A. Mesenchymal stem cell-derived extracellular vesicles for kidney repair: Current status and looming challenges. Stem Cell Res Ther 2017;8:273.

38 Tanabe K, Matsushima-Nishiwaki R, Yamaguchi S et al. Mechanisms of tumor necrosis factor-alpha-induced interleukin-6 synthesis in glioma cells. J Neuroinflam 2010;7:16.

39 Liu T, Zhang L, Joo D et al. NF-kappaB signaling in inflammation. Signal Transduct Target Ther 2017;2:17023.

40 Choi H, Lee RH, Bazhanov N et al. Anti-inflammatory protein TSG-6 secreted by activated MSCs attenuates zymosan-induced mouse peritonitis by decreasing TLR2/NF-kappaB signaling in resident macrophages. Blood 2011;118:330–338.

41 Meng Y, Eirin A, Zhu XY et al. The metabolic syndrome modifies the mRNA expression profile of extracellular vesicles derived from porcine mesenchymal stem cells. Diabetol Metab Syndr 2018;10:58.

See www.StemCellsTM.com for supporting information available online.